BIOCHEMICAL PHARMACOLOGY 75 (2008) 1797–1806

available at www.sciencedirect.com

ScienceDirect

journal homepage: www.elsevier.com/locate/biochempharm

14-3-3 protein regulates Ask1 signaling and protects against diabetic cardiomyopathy

Rajarajan A. Thandavarayan[a], *Kenichi Watanabe*[a,*], *Meilei Ma*[a], *Punniyakoti T. Veeraveedu*[a], *Narasimman Gurusamy*[b], *Suresh S. Palaniyandi*[c], *Shaosong Zhang*[d], *Anthony J. Muslin*[d], *Makoto Kodama*[e], *Yoshifusa Aizawa*[e]

[a] *Department of Clinical Pharmacology, Faculty of Pharmaceutical Sciences, Niigata University of Pharmacy and Applied Life Sciences, 265-1 Higashijima, Niigata City, Japan*
[b] *Cardiovascular Research Center, University of Connecticut School of Medicine, Farmington, USA*
[c] *Department of Chemical and Systems Biology, Stanford University School of Medicine, Stanford, USA*
[d] *Center for Cardiovascular Research, Department of Internal Medicine, Washington University School of Medicine, St. Louis, USA*
[e] *First Department of Medicine, Niigata University Graduate School of Medical and Dental Sciences, Niigata, Japan*

ARTICLE INFO

Article history:
Received 12 November 2007
Accepted 4 February 2008

Keywords:
Diabetic cardiomyopathy
14-3-3 protein
Apoptosis signal-regulating kinase 1
Thioredoxin reductase
Hypertrophy
Fibrosis
Endothelial cells

ABSTRACT

Mammalian 14-3-3 proteins are dimeric phosphoserine-binding proteins that participate in signal transduction and regulate several aspects of cellular biochemistry. Diabetic cardiomyopathy is associated with increased oxidative stress and inflammation. In order to study the pathogenic changes underlying diabetic cardiomyopathy, we examined the role of 14-3-3 protein and apoptosis signal-regulating kinase 1 (Ask1) signaling by using transgenic mice with cardiac-specific expression of a dominant-negative 14-3-3η protein mutant (DN 14-3-3η) after induction of experimental diabetes. The elevation in blood glucose was comparable between wild type (WT) and DN 14-3-3η mice. However, a marked downregulation of thioredoxin reductase was apparent in DN 14-3-3η mice compared to WT mice after induction of diabetes. Significant Ask1 activation in DN 14-3-3η after diabetes induction was evidenced by pronounced de-phosphorylation at Ser-967 and intense immunofluorescence observed in left ventricular (LV) sections. Echocardiographic analysis revealed that cardiac functions were notably impaired in diabetic DN 14-3-3η mice compared to diabetic WT mice. Marked increases in myocardial apoptosis, cardiac hypertrophy, and fibrosis were observed with a corresponding up-regulation of atrial natriuretic peptide and galectin-3, as well as a downregulation of sarcoendoplasmic reticulum Ca^{2+} ATPase2 expression. Furthermore, diabetic DN 14-3-3η mice displayed significant reductions of platelet-endothelial cell adhesion molecule-1 staining as well as endothelial nitric acid synthase and vascular endothelial growth factor expression. In conclusion, our data suggests that enhancement of 14-3-3 protein could provide a novel therapeutic strategy against hyperglycemia-induced left ventricular dysfunction and can limit the progression of diabetic cardiomyopathy by regulating Ask1 signaling.

* *Corresponding author at*: Department of Clinical Pharmacology, Faculty of Pharmaceutical Sciences, Niigata University of Pharmacy and Applied Life Sciences, 265-1 Higashijima Akiha-ku, Niigata City 956-8603, Japan. Tel.: +81 250 25 5267; fax: +81 250 25 5021.
E-mail address: watanabe@nupals.ac.jp (K. Watanabe).
0006-2952/$ – see front matter
doi:10.1016/j.bcp.2008.02.003

1. Introduction

Diabetic cardiomyopathy is now well documented and is characterized by left ventricular (LV) remodeling, which involves both diastolic and systolic dysfunction [1,2]. The development of diabetic cardiomyopathy is multifactorial and regulated by dynamic and complex mechanisms on cellular and molecular levels [3]. Hyperglycemia-induced oxidative stress is a major risk factor for the development of microvascular pathologies in the diabetic myocardium that result in myocardial cell death, hypertrophy, fibrosis, abnormalities of calcium homeostasis and endothelial dysfunction [2–4]. However, the possible molecular/genetic mechanisms involved in diabetic cardiomyopathy are not well characterized; translational studies with transgenic animals are limited and only partly explain the mechanisms of cardiomyopathy and heart failure in diabetic patients.

14-3-3 protein belongs to a class of highly conserved proteins involved in regulating apoptosis, adhesion, cellular proliferation, differentiation, survival, and signal transduction pathways [5]. Apoptosis signal-regulating kinase 1 (Ask1), a mitogen-activated protein kinase (MAPK) kinase kinase, is involved in biological responses such as apoptosis, inflammation, differentiation and survival in different cell types. Activated Ask1 relays signals to c-jun NH_2 kinase (JNK) and p38 MAPK [6,7]. Recent evidence suggests that oxidative stress activates Ask1 by dissociating its inhibitor, 14-3-3 protein, from Ask1 Ser-967 in Cos7 cells [8]. 14-3-3 protein and thioredoxin are reported to limit Ask1 activity by guarding the C-terminal and N-terminal of Ask1 kinase, respectively [9]. Moreover, Ask1 is now emerging as a potential target for cardiac diseases [10]; hence the specific role of Ask1 in the development of diabetic cardiomyopathy should be examined. We have recently reported that transgenic mice with cardiac-specific expression of a dominant-negative mutant of 14-3-3η protein (DN 14-3-3η) exhibit enhanced cardiomyocyte apoptosis, hypertrophy, and fibrosis after induction of experimental diabetes [11,12]. However, the specific involvement of the Ask1 signaling pathway in the development of diabetic cardiomyopathy has been not directly demonstrated. Based on our previous findings, we postulated that DN 14-3-3η mice could provide a model for the investigation of Ask1 signaling in the streptozotocin (STZ)-induced cardiac remodeling process.

We here demonstrate that 14-3-3 protein acts as an endogenous cardioprotector and limits the development of diabetic cardiomyopathy by limiting myocardial apoptosis, hypertrophy, fibrosis, and endothelial dysfunction via inhibition of Ask1 activation after induction of experimental diabetes.

2. Materials and methods

2.1. Generation of DN 14-3-3η transgenic mice

Transgenic DN 14-3-3η mice were generated as described previously [13]. Briefly, the coding region of human DN (R56A and R60A) 14-3-3η cDNA with a 5′-Myc-1 epitope tag was subcloned into a vector containing the α-myosin heavy chain promoter and an SV40 polyadenylation site. Linearized DNA was injected into the pronuclei of one-cell C57BL/6 XSJL embryos at the Neuroscience Transgenic Facility at Washington University School of Medicine. Progeny were backcrossed into the C57BL/6 genetic background and were analyzed by polymerase chain reaction to detect transgene integration using mouse-tail DNA as template. Age-matched C57BL/6 JAX mice (obtained from Charles River Japan Inc., Kanagawa, Japan) were used as wild type (WT) controls.

2.2. Diabetes induction

Diabetes was induced by a single intraperitoneal injection (150 mg/kg) of STZ (Sigma–Aldrich Inc., St. Loius, USA) dissolved in vehicle (20 mM sodium citrate buffer, pH 4.5) to 8–10-week-old male WT and DN 14-3-3η mice. Age-matched WT and DN 14-3-3η mice were injected with 100 μl of citrate buffer and used as non-diabetic controls. Animals were studied twice after streptozotocin administration, i.e. on day 3 for acute measurement and on day 28 for chronic measurement. Mice were maintained with free access to water and chow throughout the period of study, and animals were treated in accordance with the guidelines for animal experimentation of our institute.

2.3. Blood glucose measurement and survival rate

Blood glucose levels of animals were measured at 0, 1, 3, 7 and 28 days after STZ injection. Blood glucose level was determined using Medi-safe chips (Terumo Inc., Tokyo, Japan). Four separate groups comprised of control WT mice (vehicle treated, $n = 10$), diabetic WT mice (STZ treated, $n = 14$), control DN 14-3-3η mice (vehicle treated, $n = 10$) and diabetic DN 14-3-3η mice (STZ treated, $n = 12$) were utilized for Kaplan–Meier survival analysis.

2.4. Transthoracic echocardiography

Two-dimensional echocardiography studies were performed in anesthetized mice (pentobarbital, 50 mg/kg, i.p.) to evaluate cardiac function using an echocardiographic machine with 7.5 and 12 MHz transducers linked to an ultrasound system (SSD-5500; Aloka, Tokyo, Japan). The short-axis view of the LV was recorded to measure the LV dimension in systole (LVDs) and diastole (LVDd) as well as the percent fractional shortening (% FS). Hearts were harvested for analysis from control and diabetic mice. The LV was quickly dissected and cut into two parts. One part was immediately transferred into liquid nitrogen and then stored at −80 °C for protein analysis. The other part was either stored in 10% formalin or stored at −80 °C after the addition of Tissue-Tek OCT compound (Sakura Co. Ltd., Tokyo, Japan) for histopathological and immunohistochemical analysis.

2.5. Protein analysis

Protein lysate was prepared from heart tissue as described previously [11]. The total protein concentration in samples was measured by the bicinchonic acid method. For western blotting experiments, 100 μg of total protein was loaded and proteins were separated by SDS-PAGE (200 V for 40 min) and

electrophoretically transferred to nitrocellulose filters (semi-dry transfer at 10 V for 30 min). Filters were blocked with 5% non-fat dry milk in Tris-buffered saline (20 mM Tris, pH 7.6, 137 mM NaCl) with 0.1% Tween 20, washed, and then incubated with primary antibody. Primary antibodies employed included: rabbit polyclonal anti-Ask1 and anti-phospho (Ser-967) Ask1, mouse monoclonal anti-extracellular regulated kinase (ERK1/2) (Cell Signaling Technology Inc., MA, USA), rabbit polyclonal anti-14-3-3 (pan-14-3-3), anti-thioredoxin reductase (TrxR), anti-atrial natriuretic peptide (ANP) and anti-vascular endothelial growth factor (VEGF), goat polyclonal anti-sarcoendoplasmic reticulum Ca^{2+} ATPase2 (SERCA2) and anti-glyceraldehyde-3-phosphate dehydrogenase (GAPDH) (Santa Cruz Biotechnology Inc., CA, USA) and mouse monoclonal anti-endothelial nitric oxide synthase (eNOS) (Sigma–Aldrich) and mouse monoclonal anti-galectin-3 (Affinity Bioreagents, CO, USA). After incubation with the primary antibody, the bound antibody was visualized with horseradish peroxidase-coupled secondary antibodies (Santa Cruz Biotechnology) and chemiluminescence developing agents (Amersham Biosciences, Buckinghamshire, UK). The level of expression of each protein in control WT mice was taken as one arbitrary unit (AU). For western blotting analysis, all primary antibodies were used at a dilution of 1:1000 and secondary antibodies were used at a dilution of 1:5000. Films were scanned and band densities were quantified by densitometric analysis using Scion image software (Epson GT-X700; Tokyo, Japan).

2.6. Histopathology

Frozen LV tissues embedded in OCT compound were cut into 4-μm-thick sections and fixed in 4% paraformaldehyde (pH 7.4) at room temperature. Terminal deoxynucleotidyl transferase-meditated dUTP nick-end labeling (TUNEL) apoptosis analysis was performed as specified in the in situ apoptosis detection kit (Takara Bio Inc., Shiga, Japan) and sections were examined under light microscopy at 400-fold magnification. Paraffin-embedded sections were used for Ask1 detection using the mouse monoclonal anti-Ask1 antibody (Santa Cruz Biotechnology) followed by incubation with fluorescein isothiocyanate-conjugated secondary antibody. Capillary endothelial cells were quantified using immunohistochemical staining with the primary goat polyclonal anti-platelet-endothelial cells adhesion molecule-1 (PECAM-1) antibody (Santa Cruz Biotechnology) followed by incubation with the secondary antibody; diamino-benzidine was used as the chromogen. Slides were counterstained with hematoxylin and visualized at 400× magnification. Ten random high power fields (HPF) were quantified in a blinded manner and the number of endothelial cells was expressed as the number of capillary endothelial cells/HPF. Hematoxylin and eosin (H–E) staining was used to note the cross-sectional area of cardiomyocytes at 400× magnification. The area of myocardial fibrosis in LV tissue sections stained with Azan-Mallory was quantified using a color image analyzer (CIA-102, Olympus, Tokyo, Japan) and measuring the blue fibrotic areas as opposed to the red myocardium at 100× magnification. The results were presented as the ratio of the fibrotic area to the whole area of the myocardium [14]. Digital photographs were taken using the color image analyzer (CAI-102; Olympus, Tokyo, Japan).

2.7. Statistical analysis

Data are represented as means ± standard error (S.E.). *t*-Tests were applied wherever applicable and statistical analysis between groups was performed using one-way analysis of variance followed by Tukey's method. Differences were considered as statistically significant at $P < 0.05$.

3. Results

3.1. Blood glucose and survival rate

A marked elevation in blood glucose level (Fig. 1A) was observed at 3 days after diabetes induction and persisted throughout the study period of 28 days in both WT and DN 14-3-3η mice. Animals with blood glucose levels lower than 300 mg/dl were excluded from the study. The average blood glucose level of both groups was not statistically different throughout the study. Moreover, the survival rate was significantly reduced in DN 14-3-3η mice (3 out of 12 mice died, 75%) compared to WT mice (1 out of 14 mice died) at 28 days after STZ injection (Fig. 1B).

3.2. LV expression of pan-14-3-3, TrxR, Ask1/p(Ser-967) Ask1

LV pan-14-3-3 protein expression remained unchanged in both WT and DN 14-3-3η mice at 28 days after STZ injection

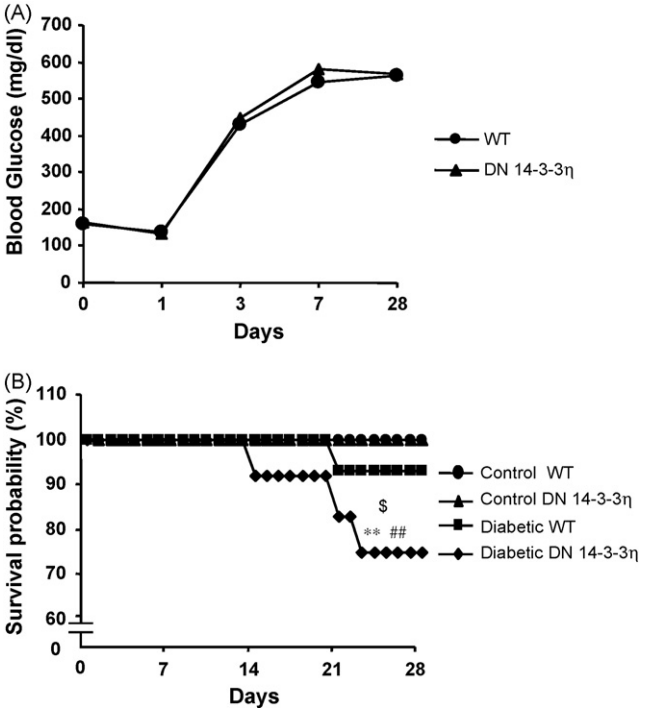

Fig. 1 – Elevated blood glucose level and decreased survival rate in diabetic WT and diabetic DN 14-3-3η mice: (A) blood glucose elevation; (B) Kaplan–Meier survival curves for STZ-treated or vehicle-treated DN 14-3-3η and WT mice. $^{**}P < 0.01$ vs. control WT mice; $^{\#\#}P < 0.01$ vs. control DN 14-3-3η mice; $^{\$}P < 0.05$ vs. diabetic WT mice on the same day.

(Fig. 2A and B). To test the influence of STZ-induced oxidative stress on the oxidoreductase system, we analyzed TrxR expression. The myocardial expression of TrxR was significantly decreased in both WT and DN 14-3-3η mice at 28 days after STZ injection (Fig. 2C and D). A more profound decrease was evident in diabetic DN 14-3-3η mice compared to diabetic WT mice. Further, we analyzed the effect of experimental diabetes and disruption of 14-3-3 protein function in the levels of Ask1 protein and phospho(Ser-967) Ask1 (indicator of active Ask1) expression in the LV. A higher expression level of Ask1 corresponded to significant de-phosphorylation at Ask1 Ser-967 in DN 14-3-3η mice relative to WT mice at 3 days after STZ injection (Fig. 2E–G). In addition, we observed intense Ask1 immunofluorescence in LV sections of DN 14-3-3η mice relative to WT mice at 28 days after STZ injection (Fig. 4B and D).

3.3. *Echocardiographic assessment of ventricular remodeling*

Intact chamber remodeling analysis by echocardiography revealed that cardiac dimensions were not different between control DN 14-3-3η and WT mice. The heart rate was similar between control WT and control DN 14-3-3η mice, and remained unchanged over the course of experimental diabetes (data not shown). However, significant increases in LVDd and

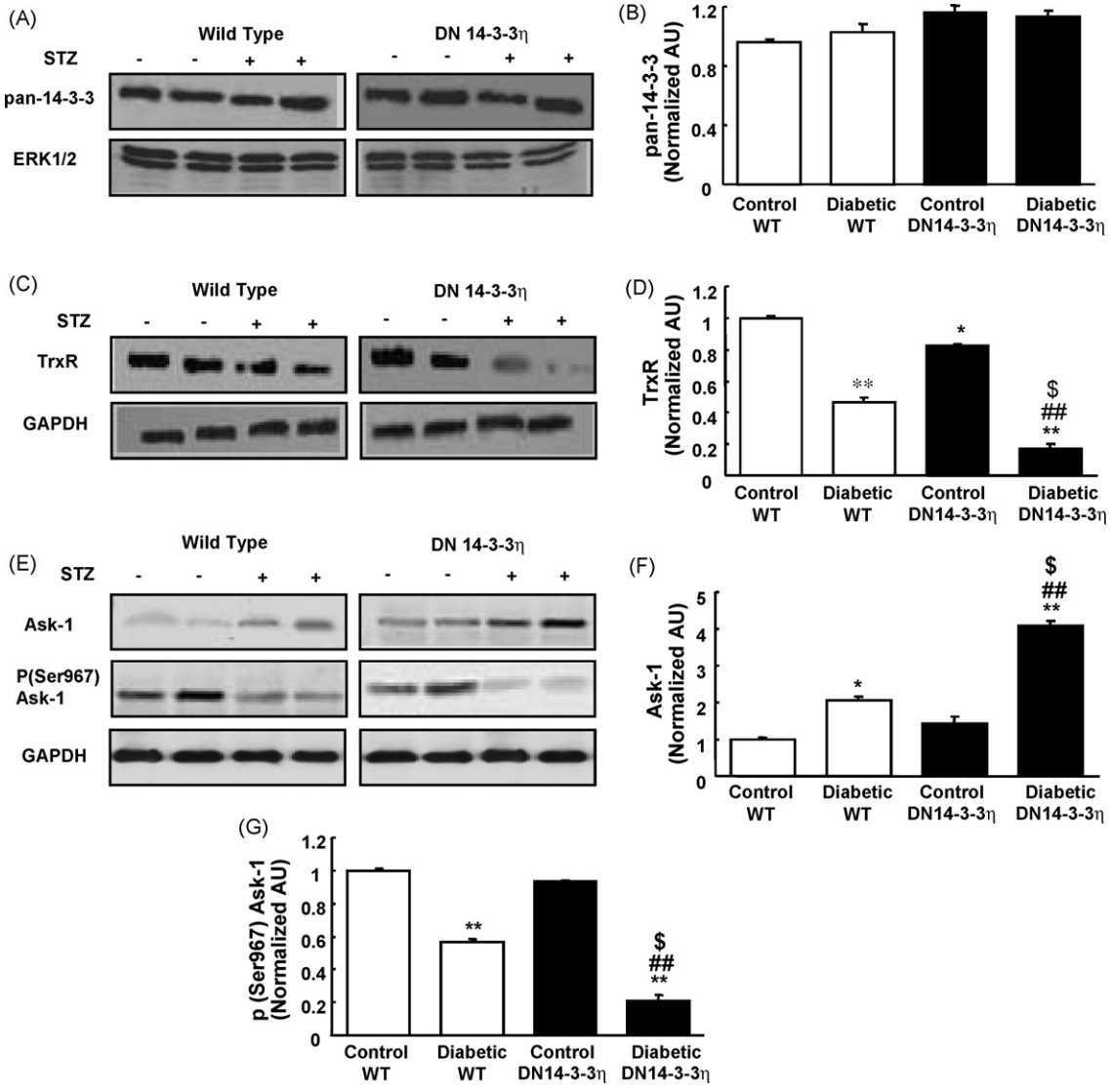

Fig. 2 – Unaltered 14-3-3 protein expression level with downregulated TrxR and dephosphorylated Ask1 after experimental diabetes: (A–D) representative western immunoblots and densitometry analysis using Scion image software for pan-14-3-3 protein (A and B) and TrxR protein (C and D) levels in control (−) and 28 days after STZ injection (+); blots were re-probed with anti-ERK1/2 or GAPDH antibodies to control for protein loading. (E–G) Ask1 activity was detected as early as 3 days after STZ injection. Ask1 antibody detects Ask1 protein expression independent of its phosphorylation state and anti-phospho(Ser-967) Ask1 antibody detects Ask1 when phosphorylated at site Ser-967; blots were normalized to GAPDH. White and black bars represent WT and DN 14-3-3η mice, respectively. Each bar represents means ± S.E. ($n = 3–4$). $^{*}P < 0.05$ vs. control WT mice; $^{**}P < 0.01$ vs. control WT mice; $^{\#\#}P < 0.01$ vs. control DN 14-3-3η mice; $^{\$}P < 0.05$ vs. diabetic WT mice on the same day.

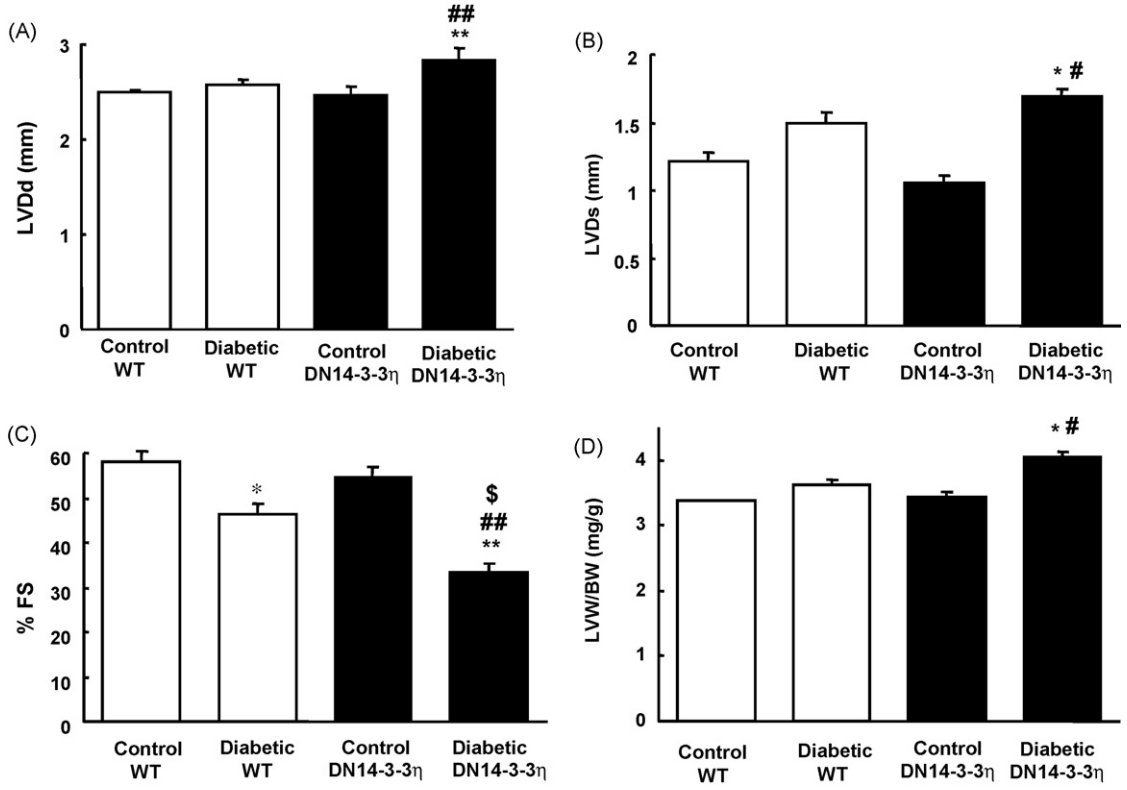

Fig. 3 – Cardiac function was evaluated using M-Mode echocardiography performed by an experienced echocardiographic analyst without knowledge of mouse genotype or previous treatment: (A) LVDd and (B) LVDs are left ventricular end-diastolic and systolic dimensions, respectively; (C) % FS; (D) morphometrically determined LVW/BW ratio. White and black bars represent WT and DN 14-3-3η mice, respectively. Each bar represents means ± S.E. ($n = 3–4$). $^{*}P < 0.05$ vs. control WT mice; $^{**}P < 0.01$ vs. control WT mice; $^{\#}P < 0.05$ vs. control DN 14-3-3η mice; $^{\#\#}P < 0.01$ vs. control DN 14-3-3η mice; $^{\$}P < 0.05$ vs. diabetic WT mice on the same day.

LVDs, and a corresponding decrease in % FS were observed in DN 14-3-3η mice at 28 days after STZ injection (Fig. 3A–C).

3.4. *Cardiac hypertrophy, interstitial fibrosis, related protein expression, and TUNEL analysis*

The average cross-sectional diameter of cardiac myocyte was slightly increased (13.4 ± 0.55 μm) in WT mice but significantly increased (16.8 ± 0.46 μm, $P < 0.05$) in DN 14-3-3η mice at 28 days after STZ injection when compared to control WT mice (11.8 ± 0.61 μm) and control DN 14-3-3η mice (11.7 ± 0.58 μm) (Fig. 4E–H). Furthermore, a marked increase in the ratio of LV weight to body weight (LVW/BW) was observed in DN 14-3-3η mice at 28 days after STZ injection (Fig. 3D). Myocardial fibrosis was concurrently elevated in both WT and DN 14-3-3η mice at 28 days after STZ injection (3.2 ± 0.59%, $P < 0.05$ and 6.5 ± 0.66%, $P < 0.01$, respectively) compared with control WT mice (1.1 ± 0.31%) and control DN 14-3-3η mice (1.2 ± 0.23%) (Fig. 4I–L). In addition, myocardial fibrosis was also significantly increased in diabetic DN 14-3-3η mice ($P < 0.05$) compared with diabetic WT mice (Fig. 4J and L). The expression of molecular markers of cardiac hypertrophy such as ANP and pro-fibrotic protein galectin-3 expression were also elevated in WT and DN 14-3-3η mice at 28 days after STZ injection (Fig. 5A–C). Myocardial expression of SERCA2 was typically decreased in DN 14-3-3η mice relative to diabetic WT mice at 28 days after STZ injection (Fig. 5A and D). The number of TUNEL-positive cells in LV sections was not different between control WT and DN 14-3-3η mice (Fig. 4M and O) and expectedly, the number of TUNEL-positive cells was increased in LV sections at 3 days after diabetes induction and was markedly higher in diabetic DN 14-3-3η mice (0.453 ± 0.035%, $P < 0.01$, Fig. 4P) compared to diabetic WT mice (0.121 ± 0.028%, Fig. 4N).

3.5. *Myocardial capillary endothelial cells, eNOS and VEGF expression*

As depicted in Fig. 6D and E, immunohistochemical staining with anti-PECAM-1 antibody revealed a significant decrease in the number of capillary endothelial cells in the LV of DN 14-3-3η mice at 28 days after STZ injection. A mild reduction in the number of capillary endothelial cells was also observed in WT mice at 28 days after STZ injection; however this effect was not statistically significant (Fig. 6B and E). To further establish a correlation and confirm our findings, we carried out western immunoblotting for eNOS protein expression in LV protein lysates and observed a significant reduction of eNOS protein expression in DN 14-3-3η mice relative to WT mice at 28 days after STZ injection (Fig. 6F and G). Furthermore, in order to clarify whether experimental diabetes and disruption of 14-3-

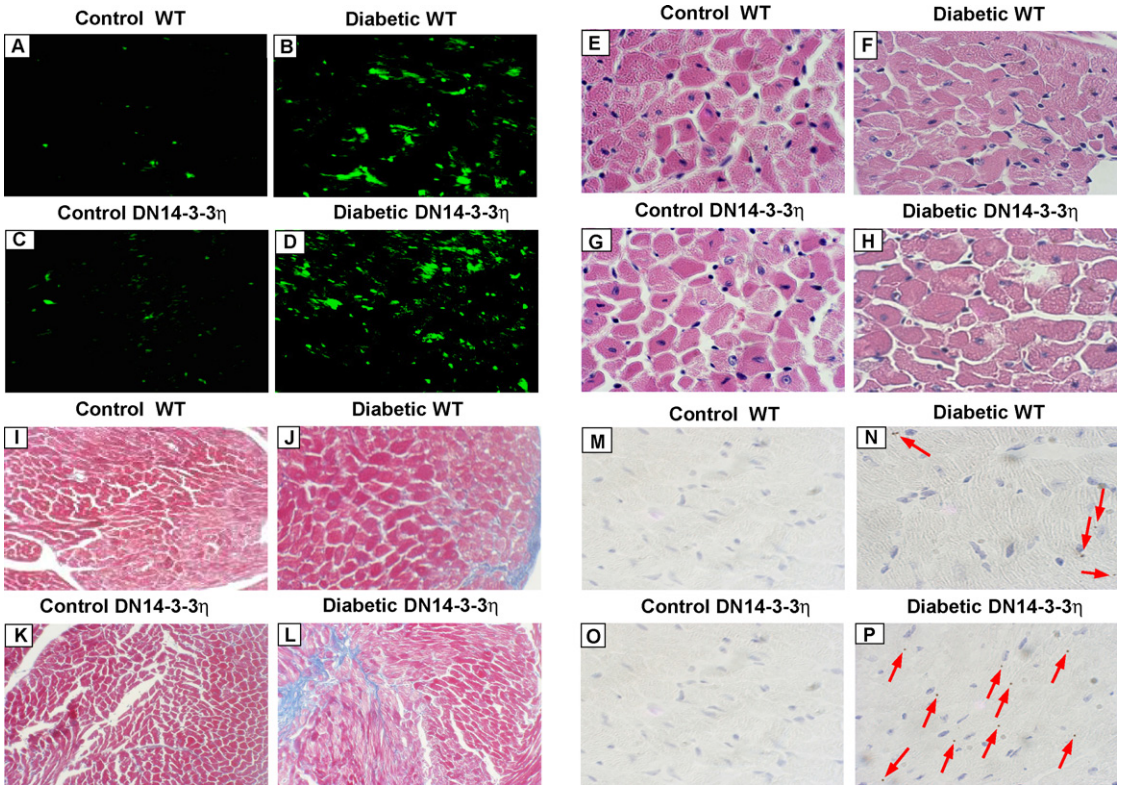

Fig. 4 – 14-3-3 protein protects against cardiac remodeling after diabetes: (A–D) representative photomicrographs of LV sections showing Ask1 immunofluorescence identified by immunohistochemical staining with anti-Ask1 antibody, (A and B) control and WT mice, respectively, (C and D) control and day-28 diabetic DN 14-3-3η mice, respectively (400×); Intense immunofluorescence was detected in LV sections of diabetic DN 14-3-3η mice. (E–H) Myocardial tissue sections stained with H–E showing cross-sectional area of cardiomyocytes in control and day-28 diabetic WT mice (E and F, respectively), as well as control and day-28 diabetic DN 14-3-3η mice (G and H, respectively) at 400× magnification. (I–L) Azan Mallory staining showing interstitial fibrosis in control and day-28 diabetic WT mice (I and J, respectively), as well as control and day-28 diabetic DN 14-3-3η mice (K and L, respectively) at 100× magnification; Note the extracellular matrix content (blue color) and disarray in day-28 diabetic DN 14-3-3η mice. (M–P) Myocardial tissue sections TUNEL stained for apoptotic nuclei (indicated by arrows) in control and day-3 diabetic WT mice (M and N, respectively), as well as control and day-3 diabetic DN 14-3-3η mice (O and P, respectively) at 400× magnification.

3 protein function affects the maintenance of vascularity, we analyzed VEGF protein expression. We found that VEGF expression was significantly reduced in DN 14-3-3η mice compared to WT mice at 28 days after STZ injection (Fig. 6F and H).

4. Discussion

In the present study we analyzed the development of diabetic cardiomyopathy in DN 14-3-3η genetically modified mice. We demonstrate that DN 14-3-3η mice exhibit an accelerated development of diabetic cardiomyopathy with a 75% survival rate and our data suggest that intact 14-3-3 protein function is crucial for the diabetic myocardium. We have previously shown that DN 14-3-3η represents 50% of total protein in the LV of DN 14-3-3η mice [13]. When mutant forms of mammalian 14-3-3η and ζ were made that were homologous to the dominant-negative forms of *Drosophila melanogaster* 14-3-3ε, they were found to have a modest reduction in their ability to bind phosphoserine-containing peptides [15–17]. In view of the fact that cellular injury upregulates 14-3-3 protein expression in certain disease conditions such as cancer [18], we tried to ascertain whether myocardial injury caused by sustained hyperglycemia could alter 14-3-3 protein expression. However, we observed no significant alteration in pan-14-3-3 protein levels over the course of the present study, indicating that neither hyperglycemic episodes nor hyperglycemia-induced DNA damage alter 14-3-3 protein expression *in vivo*. It is therefore possible that 14-3-3 protein could be a resident adaptor molecule that offers cardioprotection to the metabolically stressed myocardium.

4.1. *Ask1 expression and subsequent stress responses*

We have previously reported that myocardial apoptosis peaks in DN 14-3-3η mice at 3 days after STZ injection [11]. In this study, we observed significant enhancement of Ask1 activity in diabetic DN 14-3-3η mice on the same day. The enhanced Ask1 activity was associated with de-phosphorylation at

phospho Ask1 (Ser-967), which has been identified as the 14-3-3 protein-binding site for Ask1 after diabetes. Overexpression of 14-3-3 protein has been shown to block Ask1-induced apoptosis in HeLa cells [19] and disruption of the Ask1/14-3-3 protein interaction by oxidative stress such as H_2O_2 dramatically enhances apoptosis in COS7 cells [8]. In the same study, it was also reported that dephosphorylation of Ask1 at Ser-967 and the release of 14-3-3 protein from Ask1 correlates with increased Ask1 activity. Moreover, we previously showed enhanced activity of the downstream effector of Ask1, JNK, in DN 14-3-3η mice at 3 days after STZ injection [11]. Hence, we propose that diabetes-induced Ask1 activity mediates myocardial apoptosis by downstream activation of JNK. These findings suggest that endogenous cardiac resident 14-3-3 protein plays a crucial role in limiting Ask1–JNK-induced cardiac apoptosis in the diabetic myocardium.

Ask1 activation is shown to be regulated via oxidative stress [8]. Treatment with an antioxidant enhanced the interaction of 14-3-3 protein and thioredoxin with Ask1 [20]. TrxR is an important component of the redox regulation machinery involved in cardiac remodeling and is generally inactivated by oxidants such as H_2O_2 [21]. In this study, we showed a significant reduction of TrxR expression in LV sections after diabetes induction. In support of our results, Li et al. [4] have recently reported a similar depletion of TrxR in the diabetic myocardium. Oxidative stress in the diabetic myocardium might have caused the reduction of TrxR activity, which is much evident in DN-14-3-3η mice heart, where the level of oxidative stress is negatively correlated with the activation of TrxR. Decreased TrxR in the diabetic heart might prevent the binding of thioredoxin with Ask1. Thus, the thioredoxin-mediated control of Ask1 in the diabetic heart is diminished. On the other hand, oxidative stress causes dephosphorylation of Ser-967 of Ask1, resulting in dissociation of 14-3-3 protein from Ask1 [8]. Thus, another control of Ask1 mediated via 14-3-3 protein is diminished. We presume that oxidative stress may be the causative factor for the diminished control of Ask1 by 14-3-3 protein and thioredoxin in the diabetic heart. Since 14-3-3 protein-mediated control of Ask1 is almost totally lost in DN-14-3-3η mice, where oxidative stress further cause diminishing thioredoxin-mediated control, DN-14-3-3η mice heart may be much vulnerable to Ask1-mediated cardiac damage. It is likely that the intact 14-3-3 protein aids the oxidoreductase system in regulating oxidative stress after diabetes induction. However, the mechanism by which 14-3-3 protein and thioredoxin coordinate the control of Ask1 in response to diabetes-induced oxidative stress requires further investigation.

4.2. *14-3-3 protein/Ask1 regulates myocardial remodeling*

Ask1 is known to act downstream to Rac-1 in mediating cardiomyocyte hypertrophy [22]. In the present study we

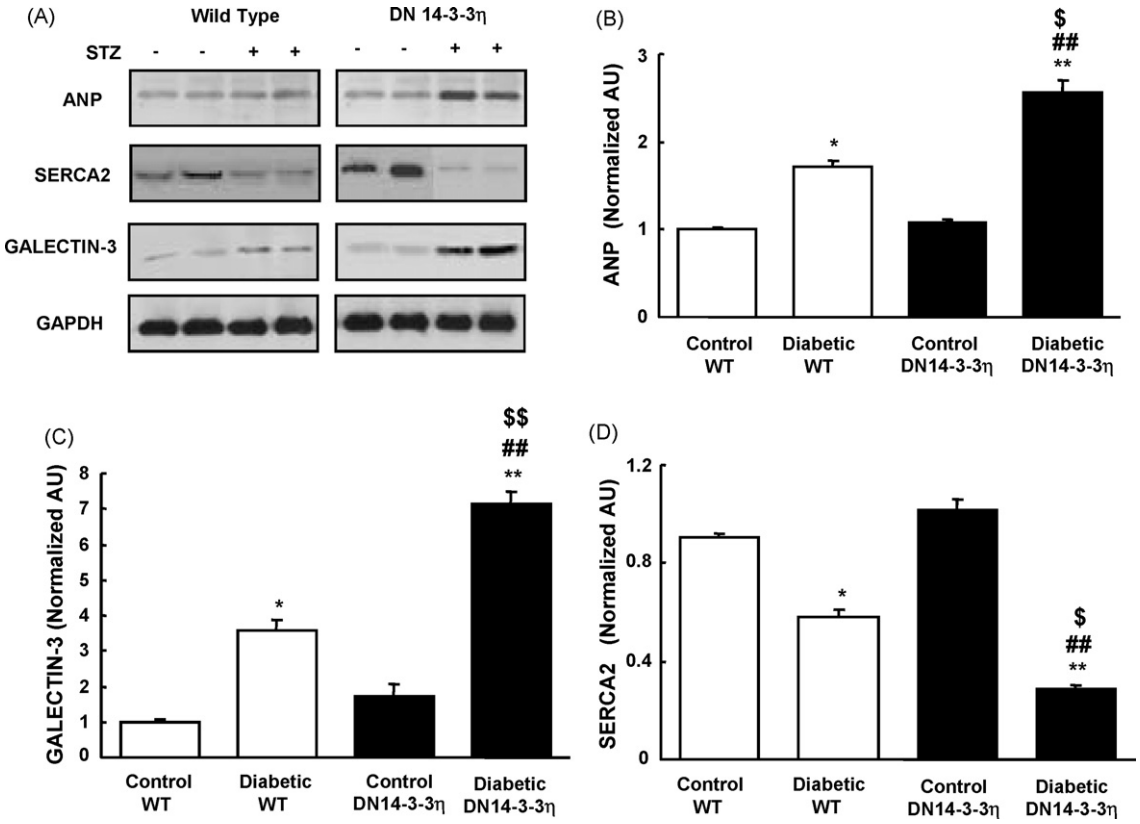

Fig. 5 – Left ventricular ANP, SERCA2, and galectin-3 expression in control and day-28 diabetic mice: (A–D) representative western immunoblots and densitometry analysis using Scion image software for ANP (A and B), galectin-3 (A and C), and SERCA2 (A and D) normalized against GAPDH. White and black bars represent WT and DN 14-3-3η mice, respectively. Each bar represents means ± S.E. (n = 3–4). $^{*}P < 0.05$ vs. control WT mice; $^{**}P < 0.01$ vs. control WT mice; $^{\#\#}P < 0.01$ vs. control DN 14-3-3η mice; $^{\$}P < 0.05$, $^{\$\$}P < 0.01$ vs. diabetic WT mice on the same day.

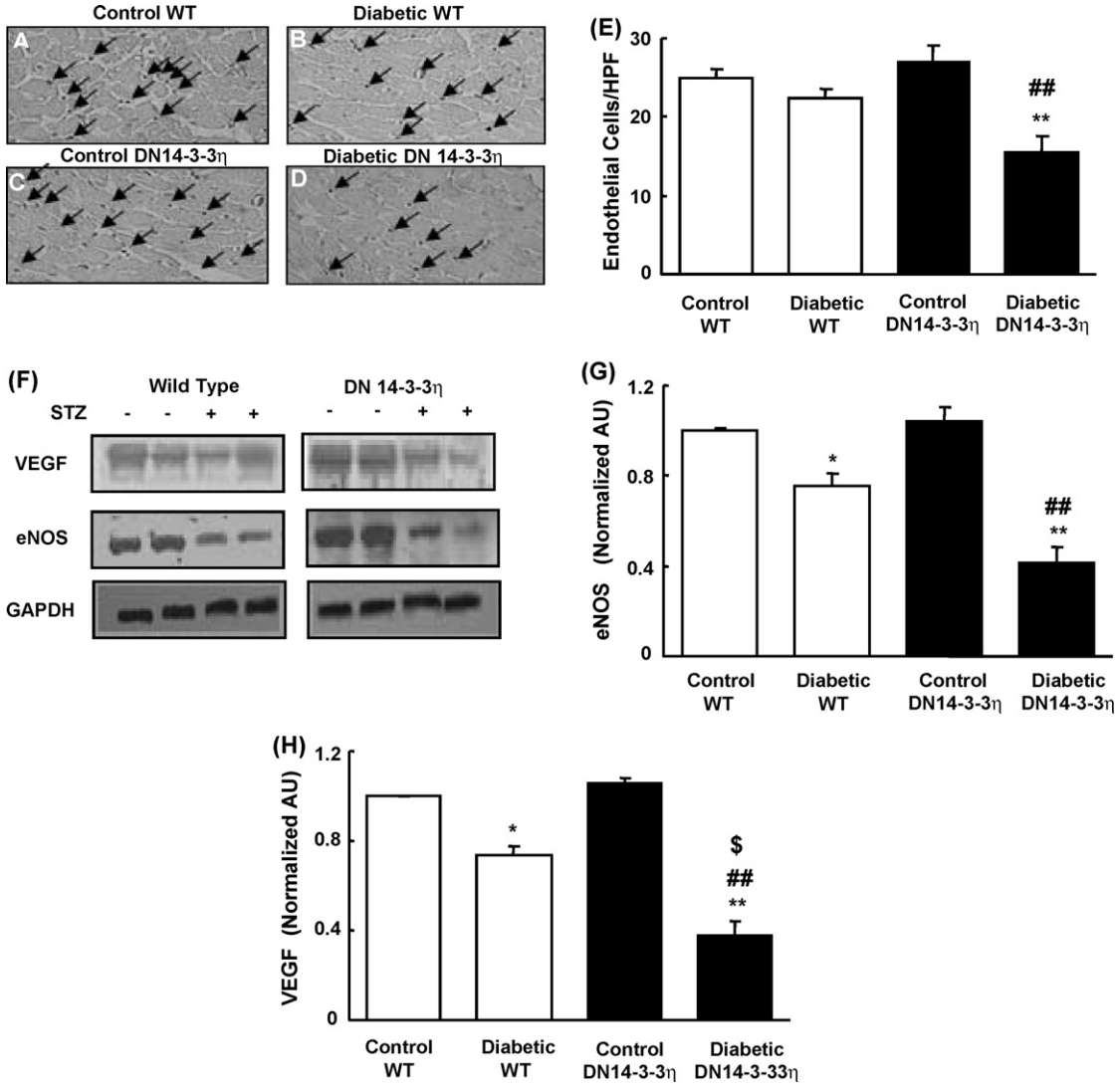

Fig. 6 – 14-3-3 protein maintains myocyte–endothelial coupling and vascularity after diabetes: (A–D) representative photomicrographs of capillary endothelial cells in the LV identified by immunohistochemical staining with anti-PECAM-1 antibody; (A and B) control and day-28 diabetic WT mice, respectively, (C and D) control and day-28 diabetic DN 14-3-3η mice, respectively. Original magnification 400×, arrows indicate PECAM-1 positive cells. (F–H) Representative western immunoblots and densitometry analysis using Scion image software for eNOS and VEGF in control and day-28 diabetic mice; blots were normalized against GAPDH. White and black bars represent WT and DN 14-3-3η mice, respectively. Each bar represents means ± S.E. (n = 3–4). $^{*}P < 0.05$ vs. control WT mice; $^{**}P < 0.01$ vs. control WT mice; $^{\#\#}P < 0.01$ vs. control DN 14-3-3η mice; $^{\$}P < 0.05$ vs. diabetic WT mice on the same day.

found intense Ask1 immunofluorescence in LV sections of diabetic DN 14-3-3η mice with significant myocyte enlargement and ANP expression. Moreover, prominent LV hypertrophy developed in diabetic DN 14-3-3η mice with distinct LV chamber dilation, decreased % FS, and increased LVW/BW, supporting our notion of 14-3-3 protein-mediated cardioprotection via Ask1 inhibition in the diabetic myocardium. Moreover, Ask1$^{-/-}$ mice were reported to be resistant to angiotensin II (Ang II)-induced hypertrophy [10], and we have also observed marked elevation in Ang II levels [23] and peak p38 MAPK phosphorylation (activation) with significant hypertrophy and fibrosis in DN 14-3-3η mice after induction of diabetes [11,12]. It is therefore possible that cardiac hypertrophy associated with diabetes may also be mediated by the Ang II–Rac–Ask1 axis.

Furthermore, Ask1 activation followed by that of p38 MAPK is reported to enhance myocardial monocyte chemoattractant protein 1 expression in cardiac fibroblasts [24] and we believe that it likely contributes to chronic tissue damage in diabetic heart disease. In our previous study we observed marked increases in collagen III and transforming growth factor β1 levels in the LV tissue of diabetic DN 14-3-3η mice [12]. A noteworthy finding of the present study is that galectin-3 levels were elevated in the LV tissue of diabetic DN 14-3-3η mice. Galectin-3 has now emerged as the most robustly overexpressed gene in failing hearts and is thought to

influence cardiac fibroblast proliferation, collagen deposition, and ventricular dysfunction [25]. Although speculative at present, it is possible that increased Ask1 activity in diabetic DN 14-3-3η mice hearts could indirectly be responsible for galectin-3 upregulation in macrophages [26]. We have also shown that Ask1 activity in diabetic DN 14-3-3η mice was associated with a more profound decrease in SERCA2 expression, which is typically downregulated in experimental diabetes [27]. MAPK kinase 6 (MKK6)–p38 MAPK signaling is reported to downregulate SERCA2 and prolong cardiac contractile calcium transients [28], implying that Ask1 may influence SERCA2 expression by acting upstream of MKK6 and p38 MAPK activation, which is exponentially enhanced by the disruption of 14-3-3 protein function [29,30].

4.3. *14-3-3 protein/Ask1 regulates endothelial–myocyte coupling and vascularity*

Previous evidence indicated a possible crosstalk in signaling pathways between cardiomyocytes and non-cardiomyocytes in the myocardium [31]. Accumulation of oxidized matrix between non-cardiomyocyte endothelial cells and cardiomyocytes is correlated with LV diastolic dysfunction that is in turn associated with diabetes [32]. We found a significant depletion of capillary endothelial cells in LV sections of diabetic DN 14-3-3η mice that was complemented by a similar decrease in myocardial eNOS expression. Laminar flow is reported to protect endothelial cells from undergoing apoptosis by preventing dissociation of Ask1/14-3-3 protein [33]. The association between 14-3-3 protein and Ask1 also seems important for maintenance of microvasculature and blood supply in the diabetic myocardium. High glucose levels suppress carbonyl chloride-induced VEGF expression in primary neonatal cardiomyocyte cultures [34]. We also found a marked decrease in VEGF expression in diabetic DN 14-3-3η mice. VEGF is a major mediator of neovascularization and is reported to be downregulated in the diabetic myocardium, resulting in impaired collateral formation. Repletion with exogenous VEGF has been reported to ameliorate diabetic cardiomyopathy [35]. High glucose-induced oxidative stress has been shown to inhibit the pro-survival effects of VEGF through p38 MAPK, which also inhibits the proliferation and migration of endothelial cells [36,37]. Our results are consistent with these findings, and we additionally highlight a possible role for Ask1 in downregulating VEGF expression through p38 MAPK after induction of diabetes. The increased number of capillary endothelial cells and higher level of eNOS level in diabetic WT mice when compared to diabetic DN 14-3-3η mice suggests that intact 14-3-3 protein function may help to maintain endothelial–myocyte coupling and vascularity in the diabetic myocardium by limiting Ask1 activity. The lack of a 14-3-3 protein overexpression experiment was a limitation of the present study that could have more strongly demonstrated the role of Ask1–14-3-3 protein in diabetic cardiomyopathy.

4.4. *Conclusion*

Our results strongly indicate that development of diabetic cardiomyopathy is accelerated after disruption of 14-3-3 protein function, in part through enhancement of the Ask1 signaling pathway. This process subsequently contributes to myocardial remodeling events such as apoptosis, hypertrophy, interstitial fibrosis, and endothelial dysfunction and aids the transition of compensated diabetic hearts to de-compensated failing hearts.

Acknowledgments

We thank Sayako Mito, Hiroka Tanaka, Flori R.S., and Wawaimuli A. for their assistance in this work. This research was supported by grants from Yujin Memorial Grant; the Ministry of Education, Culture, Sports, Science and Technology of Japan; and Promotion and Mutual Aid Corporation for Private Schools of Japan.

REFERENCES

[1] Zarich SW, Nesto RW. Diabetic cardiomyopathy. Am Heart J 1989;118:1000–12.
[2] Fang ZY, Prins JB, Marwick TH. Diabetic cardiomyopathy: evidence, mechanisms, and therapeutic implications. Endocr Rev 2004;25:543–67.
[3] Cai L, Kang YJ. Cell death and diabetic cardiomyopathy. Cardiovasc Toxicol 2003;3:219–28.
[4] Li X, Xu Z, Shuman Li, Rozanski GJ. Redox regulation of Ito remodeling in diabetic rat heart. Am J Physiol Heart Circ Physiol 2005;288:H1417–24.
[5] Wilker E, Yaffe MB. 14-3-3 proteins—a focus on cancer and human disease. J Mol Cell Cardiol 2004;37:633–42.
[6] Tobiume K, Matsuzawa A, Takahashi T, Nishitoh H, Morita K, Takeda K, et al. ASK1 is required for sustained activations of JNK/p38 MAP kinases and apoptosis. EMBO Rep 2001;2:222–8.
[7] Takeda K, Hatai T, Hamazaki TS, Nishitoh H, Saitoh M, Ichijo H. Apoptosis signal-regulating kinase 1 (ASK1) induces neuronal differentiation and survival of PC12 cells. J Biol Chem 2000;275:9805–13.
[8] Goldman EH, Chen L, Fu H. Activation of apoptosis signal-regulating kinase 1 by reactive oxygen species through dephosphorylation at serine 967 and 14-3-3 dissociation. J Biol Chem 2004;279:10442–9.
[9] Li X, Zhang R, Luo D, Park SJ, Wang Q, Kim Y, et al. Tumor necrosis factor alpha-induced desumoylation and cytoplasmic translocation of homeodomain-interacting protein kinase 1 are critical for apoptosis signal-regulating kinase 1-JNK/p38 activation. J Biol Chem 2005;280:15061–70.
[10] Izumiya Y, Kim S, Izumi Y, Yoshida K, Yoshiyama M, Matsuzawa A, et al. Apoptosis signal-regulating kinase 1 plays a pivotal role in angiotensin II-induced cardiac hypertrophy and remodeling. Circ Res 2003;93:874–83.
[11] Gurusamy N, Watanabe K, Ma M, Zhang S, Muslin AJ, Kodama M, et al. Dominant negative 14-3-3 promotes cardiomyocyte apoptosis in early stage of type I diabetes mellitus through activation of JNK. Biochem Biophys Res Commun 2004;320:773–80.
[12] Gurusamy N, Watanabe K, Ma M, Zhang S, Muslin AJ, Kodama M, et al. Inactivation of 14-3-3 protein exacerbates cardiac hypertrophy and fibrosis through enhanced expression of protein kinase C beta2 in experimental diabetes. Biol Pharm Bull 2005;28:957–62.
[13] Xing H, Zhang S, Weinheimer C, Kovacs A, Muslin AJ. 14-3-3 proteins block apoptosis and differentially regulate MAPK cascades. EMBO J 2000;19:349–58.

[14] Kato K, Nakazawa M, Masani F, Izumi T, Shibata A, Imai S. Ethanol ingestion on allylamine-induced experimental subendocardial fibrosis. Alcohol 1995;12:233–9.
[15] Thorson JA, Yu LW, Shih NY, Graves PR, Tanner JW, et al. 14-3-3 proteins are required for maintenance of Raf-1 phosphorylation and kinase activity. Mol Cell Biol 1998;18:5229–38.
[16] Wang H, Zhang L, Liddington R, Fu H. Mutations in the hydrophobic surface of an amphipathic groove of 14-3-3ζ disrupt its interaction with Raf-1 kinase. J Biol Chem 1998;273:16297–304.
[17] Rittinger GW, Budman J, Xu J, Volinia S, Cantley LC, Smerdon SJ, et al. Structural analysis of 14-3-3 phosphopeptide complexes identifies a dual role fro the nuclear export signal of 14-3-3 in ligand binding. Mol Cell 1999;4:153–66.
[18] Nakayama H, Sano T, Motegi A, Oyama T, Nakajima T. Increasing 14-3-3 sigma expression with declining estrogen receptor alpha and estrogen-responsive finger protein expression defines malignant progression of endometrial carcinoma. Pathol Int 2005;55:707–15.
[19] Zhang L, Chen J, Fu H. Suppression of apoptosis signal-regulating kinase 1-induced cell death by 14-3-3 proteins. Proc Natl Acad Sci USA 1999;96:8511–5.
[20] Kuo PL, Chen CY, Hsu YL. Isoobtusilactone A induces cell cycle arrest and apoptosis through reactive oxygen species/apoptosis signal-regulating kinase 1 signaling pathway in human breast cancer cells. Cancer Res 2007;67:7406–20.
[21] Sun QA, Wu Y, Zappacosta F, Jeang FT, Lee BJ, Hatfield DL, et al. Redox regulation of cell signaling by selenocysteine in mammalian thioredoxin reductases. J Biol Chem 1999;274:24522–30.
[22] Higuchi Y, Otsu K, Nishida K, Hirotani S, Nakayama H, Yamaguchi O, et al. The small GTP-binding protein Rac1 induces cardiac myocyte hypertrophy through the activation of apoptosis signal-regulating kinase 1 and nuclear factor-kappa B. J Biol Chem 2003;278:20770–7.
[23] Gurusamy N, Watanabe K, Ma M, Prakash P, Hirabayashi K, Zhang S, et al. Glycogen synthase kinase 3β together with 14-3-3 protein regulates diabetic cardiomyopathy: effect of losartan and tempol. FEBS Lett 2006;580:1932–40.
[24] Omura T, Yoshiyama M, Kim S, Matsumoto R, Nakamura Y, Izumi Y, et al. Involvement of apoptosis signal-regulating kinase-1 on angiotensin II-induced monocyte chemoattractant protein-1 expression. Arterioscler Thromb Vasc Biol 2004;24:270–5.
[25] Sharma UC, Pokharel S, van Brakel TJ, van Berlo JH, Cleutjens JP, Schroen B, et al. Galectin-3 marks activated macrophages in failure-prone hypertrophied hearts and contributes to cardiac dysfunction. Circulation 2004;110:3121–8.
[26] Kim K, Mayer EP, Nachtigal M. Galectin-3 expression in macrophages is signaled by Ras/MAP kinase pathway and up-regulated by modified lipoproteins. Biochim Biophys Acta 2003;1641:13–23.
[27] Depre C, Young ME, Ying J, Ahuja HS, Han Q, Garja N, et al. Streptozotocin-induced changes in cardiac gene expression in the absence of severe contractile dysfunction. J Mol Cell Cardiol 2000;32:985–6.
[28] Andrews C, Ho PD, Dillmann WH, Glembotski CC, McDonough PM. The MKK6–p38 MAPK pathway prolongs the cardiac contractile calcium transient, downregulates SERCA2, and activates NF-AT. Cardiovasc Res 2003;59:46–56.
[29] Liu Q, Wilkins BJ, Lee YL, Ichijo H, Molkentin JD. Direct interaction and reciprocal regulation between Ask1 and calcineurin-NFAT control cardiomyocyte death and growth. Mol Cell Biol 2006;26:3785–96.
[30] Munch G, Bolck B, Karczewski P, Schwinger RH. Evidence for calcineurin-mediated regulation of Serca2a activity in human myocardium. J Mol Cell Cardiol 2002;34:321–34.
[31] Harada M, Qin Y, Takano H, Minamino T, Zou Y, Toko H, et al. G-CSF prevents cardiac remodeling after myocardial infarction by activating the Jak-Stat pathway in cardiomyocytes. Nat Med 2005;11:305–11.
[32] Tyagi SC, Rodriguez W, Patel AM, Roberts AM, Falcone JC, Passmore JC, et al. Hyperhomocysteinemic diabetic cardiomyopathy: oxidative stress, remodeling, and endothelial–myocyte uncoupling. J Cardiovasc Pharmacol Ther 2005;10:1–10.
[33] Liu Y, Yin G, Surapisitchat J, Berk BC, Min W. Laminar flow inhibits TNF-induced ASK1 activation by preventing dissociation of ASK1 from its inhibitor 14-3-3. J Clin Invest 2001;107:917–23.
[34] Feng W, Wang Y, Cai L, Kang J. Metallothionein rescues hypoxia-inducible factor-1 transcriptional activity in cardiomyocytes activity in cardiomyocytes under diabetic conditions. Biochem Biophys Res Commun 2007;286:9.
[35] Yoon YS, Uchida S, Masuo O, Cejna M, Park JS, Gwon HC, et al. Progressive attenuation of myocardial vascular endothelial growth factor expression is a seminal event in diabetic cardiomyopathy: restoration of microvascular homeostasis and recovery of cardiac function in diabetic cardiomyopathy after replenishment of local vascular endothelial growth factor. Circulation 2005;111:2073–85.
[36] McMullen ME, Bryant PW, Glembotski CC, Vincent PA, Pumiglia KM. Activation of p38 has opposing effects on the proliferation and migration of endothelial cells. J Biol Chem 2005;280:20995–1003.
[37] el-Remessy AB, Bartoli M, Fulton D, Caldwell RB. Oxidative stress inactivates VEGF survival signaling in retinal endothelial cells via PI3-kinase tyrosine nitration. J Cell Sci 2005;118:243–52.